AIAA JOURNAL
Vol. 46, No. 4, April 2008

Lift of a Solid Spherical Particle Subject to Vorticity and/or Spin

E. Loth*
University of Illinois at Urbana–Champaign, Urbana–Champaign, Illinois 61801

DOI: 10.2514/1.29159

I. Introduction

ALTHOUGH the drag and gravitational forces are typically the most important to particle motion, the lift force can often be significant and can even approach the magnitude of the other two forces in some circumstances for surface spin velocities on the order of the translational particle velocity. As such, there are a number of multiphase systems in which consideration of lift is vital. The lift has been noted to be important for lateral migration in tubes (Saffman [1]), effectiveness of microcentrifuges (Heron et al. [2]), and particle deposition in boundary layers (Young and Leeming [3]). Another flowfield for which particle lift effects are important is that of the rotating bioreactor, which allows animal tissue growth under idealized conditions, similar to that obtained in microgravity conditions [4]. In many of these conditions, the particle can be considered as spherical and solid and the surrounding fluid as incompressible and Newtonian, as will be the focus of this review. However, there have been many excellent reviews on particle lift that discuss other conditions. In particular, the review by Leal [5] discussed dynamics and theoretical results for nonspherical particles, deformable particles, and particles in non-Newtonian fluids. On the subject of clean bubbles, Drew [6], Magnaudet and Eames [7], and Tomiyama et al. [8] discussed theory and models for lift in shear, rotational, and straining flows. For noncontinuum conditions, Wang [9] investigated the effect of particle spin in free-molecular flow and obtained a lift force that acted in a direction opposite to that of drag in continuum creeping-flow conditions. Recently, Volkov [10] investigated the transition between the continuum and the free-molecular regimes for spinning particles to obtain the critical Knudsen number at which particle spin did not yield lift.

To discuss solid particle lift for incompressible continuum Newtonian flow, it is helpful to first define the dimensionless parameters that influence lift, as well as the various forms of the lift coefficient. In general, the particle velocity $\boldsymbol{v}$ is defined as the translational velocity of the particle center of mass $\boldsymbol{x}_p$. The continuous-fluid velocity is generally defined in all areas of the domain unoccupied by particles. However, a hypothetical continuous-phase velocity can be extrapolated to the particle centroid and will be denoted as $\boldsymbol{u}$ and termed the "unhindered velocity." The relative velocity of the particles $\boldsymbol{w}$ is then based on the unhindered velocity (i.e., along a particle trajectory):

$$\boldsymbol{w}(t) \equiv \boldsymbol{v}(t) - \boldsymbol{u}(t) \tag{1}$$

It is important to note that $\boldsymbol{u}$ does *not* include the fluid dynamic effects resulting from the presence of the particle itself. The relative velocity may be nondimensionalized as the particle Reynolds number:

$$Re_p \equiv \frac{\rho_f |\boldsymbol{w}| d}{\mu_f} \tag{2}$$

In this expression, d is the particle diameter, ρ_f is the continuous-phase density, and μ_f is the continuous-phase viscosity. The magnitude of the continuous-phase vorticity (1/s) or the particle rotation (rad/s) is conventionally nondimensionalized as

$$\omega^* \equiv \omega_f d/w \tag{3}$$

$$\Omega_p^* \equiv \Omega_p d/w \tag{4}$$

Note that continuous-phase vorticity can be in the form of linear shear (ω_{shear}) or solid-body rotation (ω_{vortex}).

The two primary mechanisms for lift on a particle include vorticity in the continuous-fluid (Fig. 1a) and rotation of the particle (Fig. 1b). One may also consider a special combination case of "free rotation" (Fig. 1c) in which there is no torque on the particle ($\mathcal{T} = 0$) so that the particle attains an equilibrium (steady-state) spin related to the imposed shear. In all of these cases, the magnitude of the vorticity or the spin is typically expressed in terms of ω^* and Ω_p^* [Eq. (4)], which are proportional to the velocity gradient across the particle normalized by the particle's relative velocity. The lift-force magnitude can be nondimensionalized in the same manner as the drag [Eq. (1)], yielding

Eric Loth is an aerospace engineering graduate of the University of Michigan (Ph.D., 1998), Pennsylvania State University (M.S., 1985), and West Virginia University (B.S., 1983). He is currently a Professor of aerospace engineering at the University of Illinois at Urbana—Champaign, where he holds the title of Willett Faculty Scholar. Before joining the University of Illinois in 1990, he worked at the Laboratory for Computational Physics and Fluid Dynamics at the Naval Research Laboratory in Washington, D.C. His research has focused on aerodynamics, multiphase flow, and turbulence through computational and experimental investigations. This work has been funded by several government agencies (U.S. Air Force Office of Scientific Research, Defense Advanced Research Projects Agency, U.S. Department of Energy, Federal Aviation Administration, NASA, National Science Foundation, and the Office of Naval Research) and by a variety of national and international corporations and has resulted in more than 150 journal and conference paper publications. Prof. Loth is an Associate Fellow of the AIAA, and he has received a number of awards, including a NASA "Revolutionize Aviation" Team Award and a National Science Foundation Research Initiation Award.

Received 4 December 2006; revision received 23 August 2007; accepted for publication 2 November 2007.

*Professor, Aerospace Engineering, 306 Talbot Laboratory, 104 South Wright Street, Mail Code 236. Member AIAA.

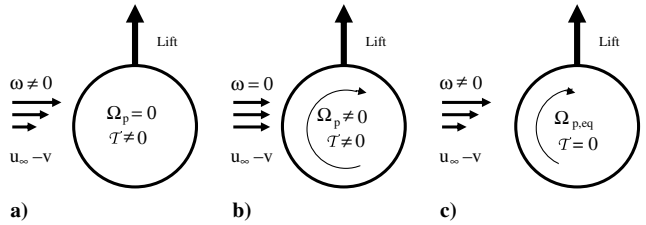

Fig. 1 Schematic of particle lift due to a) continuous-phase shear, b) particle rotation, and c) free rotation (no net torque) at particle equilibrium.

$$C_L \equiv \frac{F_L}{(\pi/8)\rho_f w^2 d^2} \tag{5}$$

The direction of the lift is defined to be perpendicular to the relative velocity (and drag), and a positive C_L is taken in the direction of $\boldsymbol{\omega}_f \times \boldsymbol{w}$ (e.g., $\boldsymbol{i}_{\omega\times w}$) for vorticity effects and in the direction of $\boldsymbol{\Omega}_p \times \boldsymbol{w}$ (i.e., $\boldsymbol{i}_{\Omega\times w}$) for particle spin effects. These directions are demonstrated in Figs. 1a and 1b, in which upward lift in both cases is associated with higher pressure on the bottom side when compared with the top side of the particle. However, certain high Re_p conditions can produce a negative C_L, as will be discussed in the following sections.

The different types of lift are often associated with the founding theories for each. For continuous-phase vorticity-induced lift, there are three types: *Saffman lift*, which is based on particles at low Re_p subjected to a linear-shear flow (Saffman), *Heron lift*, which is based on particles at low Re_p subjected to a vortex with solid-body rotation (Heron et al. [2]), and *Auton lift*, which is based on particles in inviscid flow subjected to freestream vorticity (Auton [11]). The lift associated with particles that rotate is termed herein the *Robins–Magnus lift* after experimentally observed lift of spheres by Robins in 1742 and rotating cylinders by Magnus in 1853, though the concept of sphere lift was first introduced by Newton in 1672 (Barkla and Auchterlonie [12]). In all of these cases, there can be an influence of Reynolds number, but the current understanding of such effects on lift is not as complete as in the case of drag, especially when the effects of continuous-fluid vorticity and particle rotation are combined.

II. Shear-Induced Lift

The linear-shear vorticity is defined as having a uniform gradient of the velocity in one direction (e.g., $u_x = \omega y$ and $u_y = u_z = 0$). Saffman [1] noted that there is no lift due to linear shear in the limit of creeping flow (no inertial terms). However, by including linearized inertial terms with $Re_p \ll 1$ and a weak shear based on $Re_\omega \ll 1$ (where $Re_\omega = Re_p\omega^*$), a finite lift is produced. Saffman noted that this is due to a transverse flow that extends far from the particle but is induced by the particle's surface boundary conditions. Saffman's solution [1] (Corrigendum) used a matched expansion of an inner and outer solution and the additional assumption that $Re_p \ll Re_\omega^{1/2}$, where the leading-order lift was found to be

$$\boldsymbol{F}_{L,\text{Saff}} = 1.615\mu_f w d^2 \sqrt{\frac{\omega_{\text{shear}}}{\nu_f}}\,\boldsymbol{i}_{\omega\times w} \tag{6}$$

Saffman [1] noted that two higher-order terms can be included in the following expression: $0.54\rho_f w\omega_{\text{shear}} d^3 + 0.125\rho_f \Omega_p d^3$. However, these are generally negligible in comparison, which is particularly true for a freely rotating particle ($\mathcal{T} = 0$) at low Re_p, for which $\Omega_p = \omega_{\text{shear}}/2$. Using the normalization of Eq. (5), the Saffman-lift coefficient is

$$C_{L,\text{Saff}} \equiv \frac{12.92}{\pi}\sqrt{\frac{\omega^*_{\text{shear}}}{Re_p}} \quad \text{for } Re_p \ll 1 \tag{7}$$

This form is convenient to assess the lift-to-drag ratio (via C_L/C_D). For example, the magnitude of the Saffman lift at $Re_p = 0.1$ is 5.4% of the Stokes drag magnitude. Although relatively small, this may still have a significant impact on lateral diffusion and penetration of particles in boundary-layer flows.

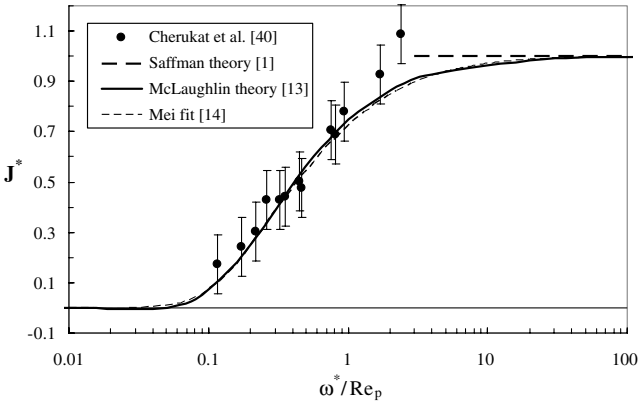

Fig. 2 Shear-induced lift theories and predictions [Eqs. (7) and (8)] assuming $Re_p \ll 1$ compared with data at $0.1 < Re_p < 1$ (Cherukat et al. [40]).

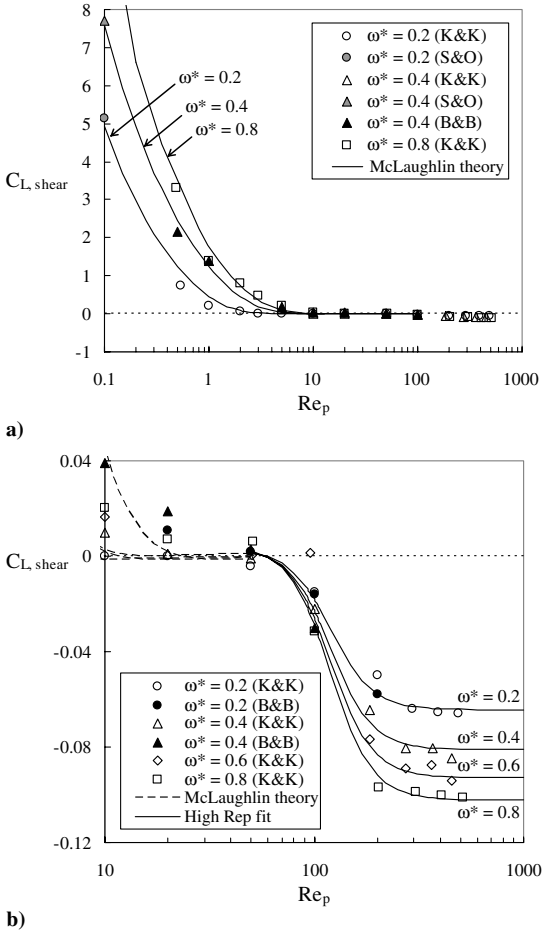

Fig. 3 Shear-induced lift as a function of Reynolds number predicted by Eqs. (9) and (10) compared with RSS results of Bagchi and Balachandar (B&B) [16] and Kurose and Komori (K&K) [15].

McLaughlin [13] extended Saffman's [1] result using Fourier analysis to eliminate the restriction of $Re_p \ll Re_\omega^{1/2}$, though again assuming small but finite values of Re_p and Re_ω. The solution yields an integral that can be numerically evaluated and the result can be described in terms of the ratio of this lift to that given by Saffman. This ratio can be defined as J^* and was empirically represented by Mei et al. [14] as

$$J^* \equiv \frac{C_{L,\mathrm{McL}}}{C_{L,\mathrm{McLSaff}}} \approx 0.3\left\{1+\tanh\left[\frac{5}{2}\left(\log_{10}\sqrt{\frac{\omega^*_{\mathrm{shear}}}{Re_p}+0.191}\right)\right]\right\} \times \left\{\frac{2}{3}+\tanh\left[6\sqrt{\frac{\omega^*_{\mathrm{shear}}}{Re_p}-1.92}\right]\right\} \quad (8)$$

The McLaughlin [13] lift ratio and the Mei et al. [14] approximating function are shown in Fig. 2, in which it can be seen that the latter is quite reasonable. It can also be seen that the lift ratio tends to unity at large values of $\omega^*_{\mathrm{shear}}/Re_p$, consistent with Saffman's [1] solution. At small values of $\omega^*_{\mathrm{shear}}/Re_p$, the predicted J^* becomes less than unity, which is consistent with experiments and resolved-surface simulations (RSS). This reduction in effectiveness is due to convection effects that diminish the far-field influence of the surface conditions. Eventually, J^* becomes negligible and even slightly negative. In this condition, the Mei et al. [14] fit is not as accurate and the higher-order terms neglected in Eq. (6) can become significant. However, the total lift will tend to be a very small fraction of the drag force for this condition, and so the Mei et al. approximation is quite reasonable for most conditions.

For finite Re_p conditions, much of the recent understanding has come from RSS results, because experiments are quite difficult. As shown in Fig. 3, the McLaughlin [13] lift force (derived for $Re_p \ll 1$) turns out to be reasonable even for $Re_p < 50$, because the RSS lift is also very small in this range. However, higher Reynolds numbers can result in a significant negative lift coefficient. Kurose and Komori [15] were the first to fully recognize this numerically and experimentally. They attributed the result to flow separation, which causes both pressure and viscous contributions to reverse the direction of lift. In particular, two separation regions were observed on the rear side of the sphere, and so the top-to-bottom rear pressure distribution was comparable and the downward pressure on the upper fore surface caused the change in lift direction. This yielded a small negative lift coefficient at high Re_p values (Fig. 3b). The simulation results of Bagchi and Balachandar [16] can be fairly well correlated with the McLaughlin [13] theory before flow separation and an empirical fit for significant separation:

$$C_{L,\mathrm{shear}} \approx C_{L,\mathrm{McL}} = J^* C_{L,\mathrm{Saff}} \quad \text{for } Re_p \le 50 \quad (9)$$

$$C_{L,\mathrm{shear}} \approx -(\omega^*_{\mathrm{shear}})^{1/3}\left\{0.0525 + 0.0575\tanh\left[5\log_{10}\left(\frac{Re_p}{120}\right)\right]\right\} \quad \text{for } Re_p > 50 \quad (10)$$

Although these expressions yield fair agreement for the lift of nonrotating solid spherical particles in an unbounded sheared domain based on simulation data, they should be used with some caution, because no quantitative experimental data are available at finite Re_p.

If the continuous-phase vorticity is defined by a vortex with solid-body rotation (e.g., $u_x = y\omega/2$, $u_y = -x\omega/2$, and $u_z = 0$), the lift is different when compared with that for linear shear. In the limit of small but finite Re_p, Heron et al. [2] showed that the theoretical lift coefficient is

$$C_{L,\mathrm{vortex}} = 5.091\sqrt{\frac{\omega^*_{\mathrm{vortex}}}{Re_p}} \quad \text{for } Re_p \ll 1 \quad (11)$$

This result is about 24% larger than that for the Saffman lift [Eq. (7)]. As shown in Fig. 4, the vortex-induced lift gives surprisingly reasonable results for Reynolds numbers as high as 100. In the inviscid limit, there is no distinction between rotational vs linear-shear lift, and Auton [11] showed the lift to be given by

$$C_{L,\mathrm{Auton}} = \frac{2\omega^*}{3} \quad (12)$$

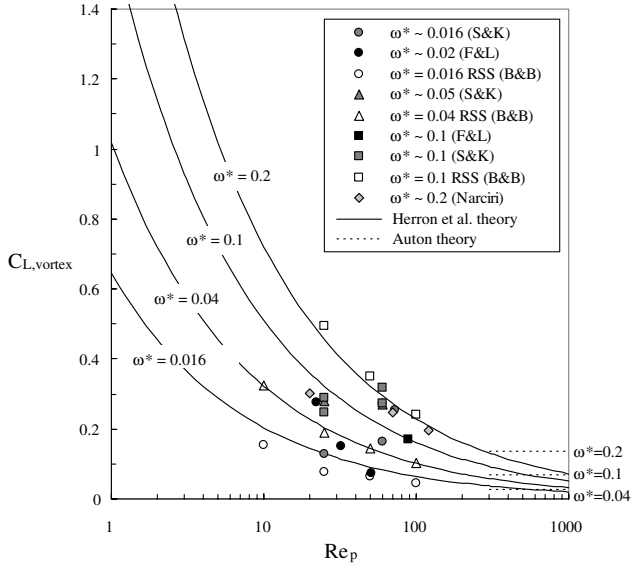

Fig. 4 Theoretical lift in a vortex solid-body rotation vortex of Herron et al. [2] for $Re_p \ll 1$ [Eq. (11)] and Auton [11] inviscid lift coefficient [Eq. (12)] compared with bubble data of Narciri [41], Sridhar and Katz (S&K) [35], and Felton and Loth (F&L) [42] as well as RSS of solid spheres by Bagchi and Balachandar (B&B) [43].

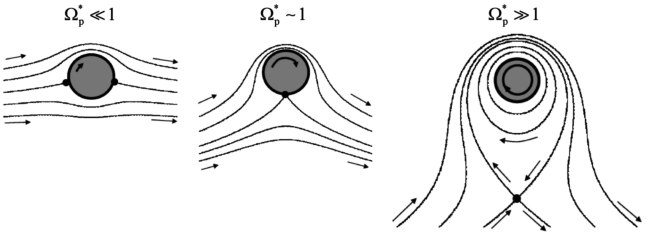

Fig. 5 Schematic of continuous-fluid streamlines for various spin rates based on inviscid flow circulation of a cylinder.

The available data are primarily for contaminated bubbles (which tend to behave like solid particles) and it appears that the lift may tend to the Auton [11] limit at higher Re_p (or depart from the Auton limit and become negative, as was the case for solid particles in linear shear). However, some of the measured lift values in this figure can be associated with the spin of the bubbles, which may be significant at high Re_p values, and so more studies are needed.

III. Spin-Induced Lift

As previously noted, the lift associated with particles that rotate is termed the Robins–Magnus lift. Unfortunately, there is no closed-form potential-flow solution for a spinning sphere. The streamlines for a spinning cylinder (Fig. 5) are qualitatively representative of the flow observed for a spinning particle if no boundary layers, flow separation, or other viscous effects are included. At low spin rates, the stagnation points tend to move downward and the higher velocities on the top lead to lower pressures and an upward lift force (in the direction of $\boldsymbol{i}_{\Omega\times w}$). As the circulation tends toward unity, the stagnation points approach each other on the bottom of the surface and the effect is exaggerated. At higher rotation rates, a closed-streamline region surrounds the particle and eventually only closed streamlines will remain in the limit of no relative velocity ($\boldsymbol{\Omega}^*_p \to \infty$). For small but finite Re_p (linearized Navier–Stokes equation), Rubinow and Keller [17] obtained the analytic solution assuming small spin rates ($\Omega^* \ll 1$). The velocity field is a linear combination of the Oseen solution and that due to a rotating sphere in a fluid at rest at infinity, which is $u_\theta = \Omega r_p (r_p/r)^3$. The resulting Robins–Magnus lift force obtained by Rubinow and Keller is given as

$$\boldsymbol{F}_{L,\Omega} = \pi \mathrm{r}_p^3 \rho_f (\boldsymbol{\Omega}_p \times \boldsymbol{w}) \quad (13)$$

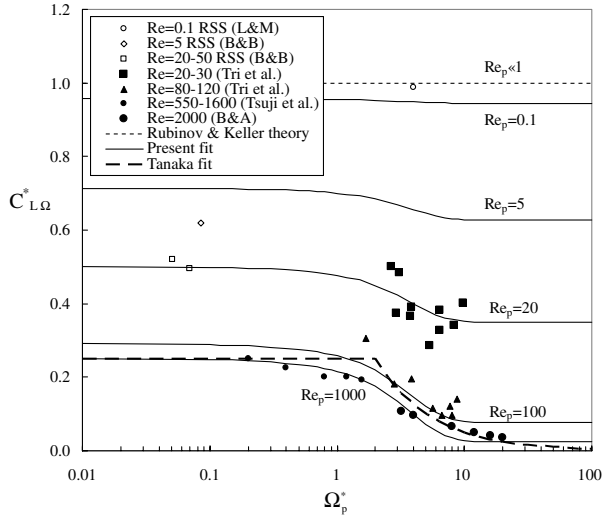

Fig. 6 Spin lift-force coefficient predictions [Eqs. (14–16)] for small and intermediate Reynolds number (approximately $Re_p < 2000$) compared with data of Bagchi and Balachandar (B&B) [16], Barkla and Auchterlonie (B&A) [12], Legendre and Magnaudet (L&M) [48], Tri et al. [19], and Tsuji et al. [44] for $a_p = 0.06$ and $a_p = 0.25$.

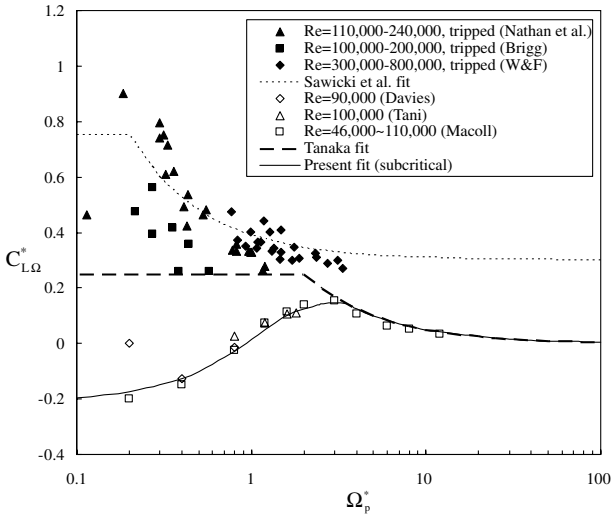

Fig. 7 Spinning particle lift coefficient predictions [Eqs. (15), (17), and (18)] for solid particles at high Reynolds numbers ($Re_p > 40,000$), based on the data of Nathan et al. [49], Briggs [50], Watts and Ferrer (W&F) [51], Davies [21], Macoll [20], and Tani [52].

Based on Eqs. (4) and (5), the associated lift coefficient becomes $C_{L,\Omega} = \Omega_p^*$, which is independent of viscosity (unlike the Saffman lift). This is based on a no-slip condition, which is appropriate for solid particles and contaminated fluid particles. The stress-free conditions associated with a pure bubble or drop can be expected to produce negligible lift in comparison.

As already mentioned, there is no inviscid solution for a sphere that satisfies the spinning surface boundary condition. Therefore, the Rubinow and Keller [17] solution is the only available theory for this flow, and we introduce a normalized spin lift coefficient accordingly; that is,

$$C_{L\Omega}^* \equiv \frac{C_{L,\Omega}}{\Omega_p^*} = 1 \quad \text{for } Re_p \ll 1 \tag{14}$$

To consider the lift beyond the Rubinow and Keller [17] regime of applicability (i.e., $Re_p > 0.1$ and $\boldsymbol{\Omega}_p^* > 0.1$), one must rely on measurements and resolved-surface simulations. Such results are shown in Fig. 6 for $Re_p < 2000$, in which it can be seen that increasing Re_p tends to reduce the lift coefficient and there is an additional, but weaker, reduction as Ω^* increases. An empirical model that gives fair agreement for high Re_p is that of Tanaka et al. [18]:

$$C_{L\Omega,\text{Tanaka}}^* = \min[0.25, 0.5/\Omega_p^*] \tag{15}$$

Other proposed models, not shown, assume that this lift coefficient is simply a constant: for example, $C_{L\Omega}^* = 0.4$ (Tri et al, [19]) or $C_{L\Omega}^* = 0.55$ (Bagchi and Balachandar [16]), which are reasonable for Re_p values of 20–120 at low and high spin rates, respectively. The present fit shown in Fig. 6 is given by

$$C_{L\Omega}^* = 1 - \{0.675 + 0.15(1 + \tanh[0.28(\Omega_p^* - 2)])\} \times \tanh[0.18\, Re_p^{(1/2)}] \tag{16}$$

This provides a more robust prediction in terms of both Re_p (up to 2000) and Ω_p^* (up to 20) and also approaches the theoretical limit for small Reynolds numbers [Eq. (13)]. As with the drag coefficient, these lift correlations for $Re_p > 200$ represent the time-averaged component, because force unsteadiness results from the unsteady separated wake region.

At much higher Reynolds numbers (greater than 50,000), the results can be grouped into two categories, as shown in Fig. 7: subcritical (where the surface is smooth and laminar separation occurs) and supercritical (where the surface is rough, tripped, or at a high enough Re_p to ensure turbulent transition before separation). Regarding the subcritical conditions, the high Ω_p^* trends are reasonably described by Eqs. (15) and (16). However, there is a curious reversal of lift direction at low spin rates, leading to negative lift coefficients. This was first observed by Maccoll [20] and later discussed by Davies [21], who related it to differences in flow separation between the top and the bottom, though this effect is still not clearly understood. A reasonable fit for the overall trend at subcritical conditions is given by

$$C_{L\Omega,\text{sub}}^* = \min[0.25\tanh(\Omega_p^* - 0.5) - 0.1, 0.5/\Omega_p^*] \tag{17}$$

For supercritical conditions, low-spin-rate lift coefficients tend toward the Rubinow and Keller [17] limit, indicating high lift generation owing to wake deflection, whereas high spin rates tend toward the subcritical limit. The data include substantial scatter, but a reasonable fit is that proposed by Sawicki et al. [22] for baseballs:

$$C_{L\Omega,\text{sup}}^* = \min[0.75, 0.3 + 0.09/\Omega_p^*] \tag{18}$$

The appearance of negative lift for high but subcritical Re_p values may be related to the rapid increase in wake volume and the onset of three-dimensional unsteady rotation of the upstream separation point, which both begin at an Re_p of about 1300. This separation behavior persists and the wake rotates around the sphere at the shedding frequency until the critical transition point (Re_p of about 300,000) [23]. After this point, the boundary-layer transitions to turbulence and the wake volume drastically reduces, because the separation point (angle measured from the front stagnation point) moves aft (from approximately 80 to 120 deg). This reattachment may be the reason for the return to positive lift.

IV. Lift and Torque for Combined Shear and Spin

In this section, the consequence of combined spin and shear will be considered in terms of particle lift and the resulting particle torque for nonequilibrium conditions. This is followed by a discussion of torque-free equilibrium spin rates and the resulting lift. Saffman [1] showed that the theoretical particle spin lift of Rubinow and Keller [17] can be linearly combined with the first-order shear-induced lift assuming $Re_p \ll 1$, $Re_\omega \ll 1$, $Re_p \ll Re_\omega^{1/2}$, and $\Omega_p^* \ll 1$. Thus, the lift force in vector form is simply the sum of Eqs. (6) and (13) so that the corresponding lift coefficient (assuming spin and shear are both perpendicular to the relative velocity and yield a positive lift) is given by

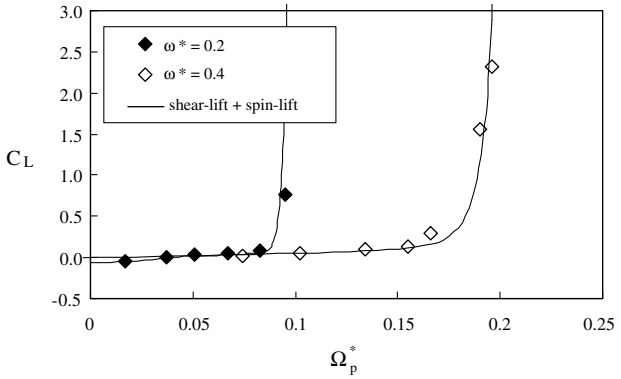

Fig. 8 Lift-force coefficient for particles under both spin and shear based on the data of Bagchi and Balachandar [16] and predictions that are a linear combination of shear-based and spin-based lift [Eqs. (7–10), (16), and (20)].

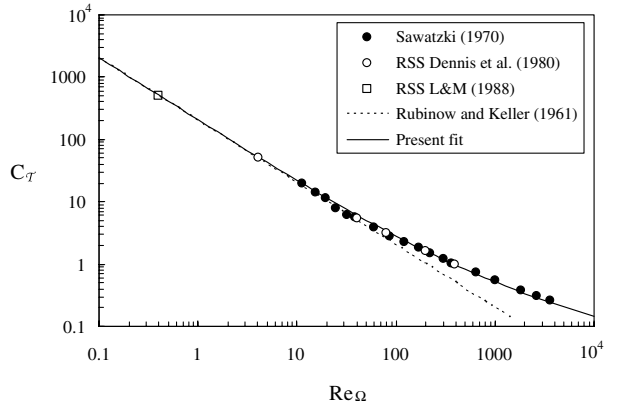

Fig. 9 Particle torque coefficient predictions [Eqs. (26c) and (27)] as a function of the spin Reynolds number for zero relative velocity ($Re_p = 0$) in a quiescent fluid ($Re_\Omega = 0$).

$$C_L = \frac{12.92}{\pi}\sqrt{\frac{\omega^*_{\text{shear}}}{Re_p}} + \Omega^*_p \quad \text{for } Re_p \ll 1 \tag{19a}$$

For small Reynolds numbers and Ω^*_p on the order of ω^*, the shear-induced (Saffman) lift will dominate the spin-induced (Robins–Magnus) lift. Note that this form is analytically exact and does *not* include the relative spin rate as suggested by Crowe et al. [24].

Salem and Oesterle [25] showed that this expression can be extended to include particle spin conditions, in which $Re_p \gg Re_\omega^{1/2}$ by simply the McLaughlin [13] correction of Eq. 6.110. Additionally, incorporating finite Re_p effects from Eq. 6.120 for the spin lift yields

$$C_L = \frac{12.92}{\pi} J^* \sqrt{\frac{\omega^*_{\text{shear}}}{Re_p}} + \Omega^*_p C^*_{L\Omega} \tag{19b}$$

Based on Figs. 3 and 6, this expression may be expected to be reasonable for $Re_p < 50$. Consistent with this, Bagchi and Balachandar [16] and others proposed that this simple linear combination could be employed for Reynolds numbers as well as nondimensional shear rates and spin rates that were no longer much less than unity; that is, the lift for combined fluid shear and particle spin can be given as

$$\begin{aligned}\boldsymbol{F}_L(\omega_{\text{shear}} \neq 0, \Omega_p \neq 0) &\approx \boldsymbol{F}_{L,\text{shear}}(\omega_{\text{shear}} \neq 0, \Omega_p = 0) \\ &+ \boldsymbol{F}_{L,\text{spin}}(\omega_{\text{shear}} = 0, \Omega_p \neq 0)\end{aligned} \tag{20}$$

This assumption, although only strictly valid in the Saffman [1] regime, was found to be reasonable based on RSS results for ω^*_{shear} and Ω^*_p values as high as 0.4 and Re_p values as high as 100, as demonstrated in Fig. 8.

To employ the spin-induced lift for a free particle, one must keep track of the instantaneous spin rate. To do this, a point-force approximation to the angular momentum of the particle can be constructed to relate particle rotation to surface torque $\mathcal{T}$ and angular moment of inertia about the centroid I_Ω along the particle path. The rotational equation of motion specifies that the rate of change of angular momentum is equal to the sum of torques acting on the particle:

$$\frac{\mathrm{d}\Delta(I_\Omega \Omega_p)}{\mathrm{d}t} = \mathcal{T}_{\text{surf}} + \mathcal{T}_{\text{coll}} \tag{21}$$

The collisional torque $\mathcal{T}_{\text{coll}}$ includes the effects of other particles or walls coming into *contact* with the particle and will not be discussed herein. The surface torque $\mathcal{T}_{\text{surf}}$ is the sum of moments associated with the surrounding *fluid stress* on the particle surface. If the particle is spherical and has uniform density, then the moment of inertia is given by

$$I_\Omega = \frac{m_p d^2}{10} \tag{22}$$

Neglecting collision interactions, the surface torque was derived by Happel and Brenner [26], who assumed weak acceleration, but allowed for a finite relative rotation with respect to fluid vorticity $\boldsymbol{\Omega}_{p,\text{rel}}$ and obtained

$$\boldsymbol{\Omega}_{p,\text{rel}} \equiv \boldsymbol{\Omega}_p - \boldsymbol{\omega}_f/2 \tag{23a}$$

$$\mathcal{T}_{\text{surf}} = -\pi\mu_f d^3 \boldsymbol{\Omega}_{p,\text{rel}} \tag{23b}$$

As such, the spin equilibrium for creeping-flow conditions corresponds to $\boldsymbol{\Omega}_{p,\text{rel}} = 0$; that is,

$$\boldsymbol{\Omega}_{p,\text{eq}} = \frac{\boldsymbol{\omega}_f}{2} \tag{24}$$

To extend the preceding to finite Reynolds numbers, we can use the suggestion of Salem and Oesterle [25] that the components can be still be linearly added but are individually modified due to a finite Reynolds number; that is,

$$\mathcal{T}_{\text{surf}} = -\pi\mu_f d^3 (f_\Omega \boldsymbol{\Omega}_p - 1/2 f_\omega \boldsymbol{\omega}_f) \tag{25}$$

This form introduces a spin correction factor f_Ω and a vorticity correction factor f_ω, both of which are simply unity for $Re_p \ll 1$. These correction factors are often defined in terms of torque coefficients and Reynolds numbers (e.g., for the spin condition):

$$C_\Omega \equiv 64\pi f_\Omega / Re_\Omega \tag{26a}$$

$$Re_\Omega \equiv \frac{\rho_f d^2 |\boldsymbol{\Omega}_p|}{\mu_f} \tag{26b}$$

$$C_{\Omega,\text{R\&K}} \equiv 64\pi / Re_\Omega \quad \text{for } Re_\Omega \ll 1 \tag{26c}$$

In this last expression, $C_{\Omega,\text{R\&K}}$ is the coefficient of torque based on the Rubinow and Keller [17] theory ($f = 1$). Results from experiments and several RSS studies with $\omega_f = 0$ have shown that this solution is reasonable for Re_Ω as high as 30. As the rotational Reynolds number increases further (up to 2000), an empirical correlation can be proposed that gives reasonable correlation with the results shown in Fig. 9

$$f_\Omega = 1 + \frac{5}{64\pi} Re_\Omega^{0.6} \tag{27}$$

This expression was obtained for $Re_p = 0$, but is also reasonable for $Re_p < 20$ based on RSS results of Salem and Oesterle [25]. An expression for the vorticity correction, at least at equilibrium

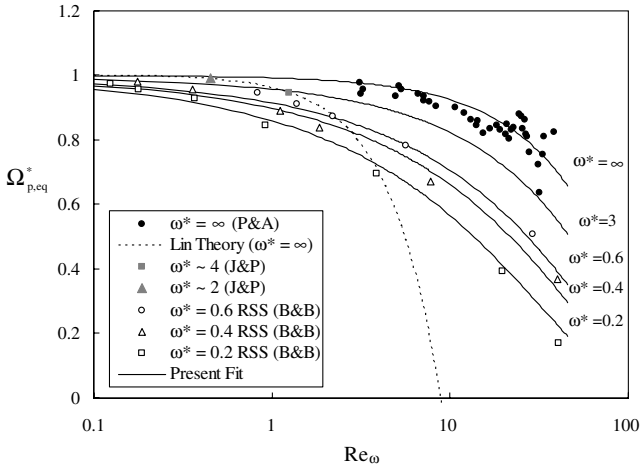

Fig. 10 Equilibrium (torque-free) particle rotation predictions [Eqs. (29) and (30)] and comparison with data from Jeffrey and Pearson [45] and Poe and Acrivos [46], as well as RSS from Bagchi and Balachandar [16].

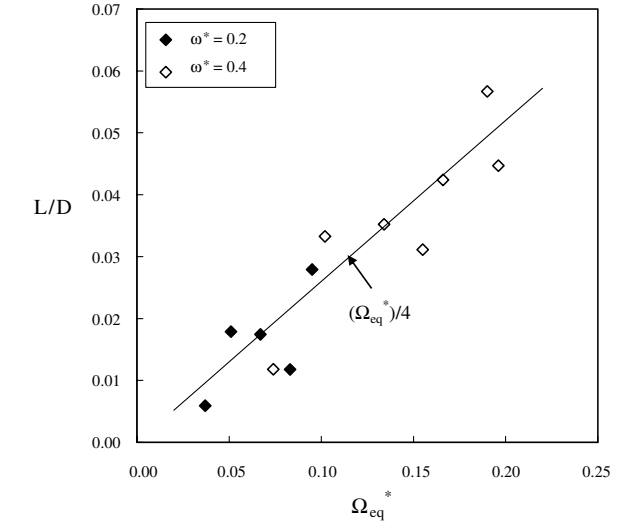

Fig. 11 Lift-to-drag ratio for particles spinning in a shear flow at equilibrium conditions based on the data of Bagchi and Balachandar [16].

conditions ($f_{\omega,eq}$) can be estimated for this same Re_p range by considering the torque-free condition as discussed next.

If there are no external torques applied to a spherical particle and it observes a steady vorticity field for long times ($t \gg \tau_\Omega$), the particle will come to an equilibrium ($\mathcal{T}_{surf} = 0$) spin rate defined as $\Omega_{p,eq}$. For finite Re_p, the normalized equilibrium spin can be expressed in terms of the creeping-flow torques via Eq. (25):

$$\Omega^*_{p.eq} \equiv \frac{\Omega_{p,eq}}{\omega_f/2} = \frac{f_\omega}{f_\Omega} \tag{28}$$

The Oseen-like first-order correction associated with finite spin Reynolds numbers but no relative velocity ($Re_\Omega \ll 1, Re_p = 0$) was obtained by Lin et al. [27] as

$$\Omega^*_{p,eq} = 1 - 0.0385\, Re_\Omega^{3/2} \tag{29}$$

However, measurements for finite Re_Ω with $Re_p = 0$ (Poe and Acrivos [46]) indicate that the reduction in $\Omega^*_{p,eq}$ is less severe, a result that is consistent with rotating cylinders in a shear flow. These trends combined with finite Re_p data are shown in Fig. 10, along with an empirical model for the equilibrium spin rate given by

$$\Omega^*_{p.eq} = (1 - 0.0075\, Re_\Omega)(1 - 0.062\, Re_p^{0.5} - 0.001\, Re_p) \tag{30}$$

The lift at equilibrium conditions may thus be obtained by substituting ω and the associated Ω_{eq} from Eq. (29) into Eq. (20), as was done for Fig. 6. For solid particles at low Re_p, the shear-based lift will dominate based on Eq. (19). However, the shear-based lift becomes weak at higher Re_p, such that the spin-based lift will be substantial (if not dominant) in comparison.

It is also interesting to compare the lift and drag forces at spin equilibrium. The simulation results for $Re_p < 40$ indicate a trend that can be approximated as $L/D \sim \Omega^*_{p,eq}/4$ (Fig. 11), suggesting that lift may only be reasonably neglected for $\Omega^*_{p,eq} \ll 1$. Finally, one may also obtain f_ω at equilibrium conditions based on the results correlated by Eq. (30) by recalling that $f_\Omega \approx 1$ for $Re_p \leq 20$ (Salem and Oesterle [25]), so that from Eq. (28), $f_{\omega,eq} \approx \Omega^*_{p,eq}$. The torque correction can then be expressed in terms of particle and shear Reynolds numbers as

$$f_{\omega,eq} \approx \frac{1 - 0.062\, Re_p^{0.5} - 0.001\, Re_p}{1 + 0.00375\, Re_{\omega,eq}(1 - 0.062\, Re_p^{0.5} - 0.001\, Re_p)} \tag{31}$$

However, more data are needed to understand the behavior at higher Re_p (greater than 20) and whether this form is reasonable for conditions other than spin equilibrium.

V. Unsteady Lift

The effects of particle acceleration or deceleration relative to the surrounding flow is well known to influence the particle drag. The influence for Stokesian conditions ($Re_p \ll 1$) was obtained theoretically by Bassett [28]. Coimbra and Kobiyashi [29] similarly derived a similar unsteady component for the lift force for the limits imposed by Saffman [1] (linearized inertial terms with $Re_p \ll 1$ and a weak shear based on $Re_\omega \ll 1$). The combination of steady lift [Eq. (6)] and unsteady lift can be written as

$$\boldsymbol{F}_L = 1.615 d^2 \sqrt{\frac{\mu_f \rho_f}{\omega}}(\boldsymbol{\omega} \times \boldsymbol{w}) + 1.615 \frac{\rho_f d^3}{2\sqrt{\omega\pi}} \left[\int_0^t \left\{ \frac{\mathrm{d}(\boldsymbol{\omega} \times \boldsymbol{w})/\mathrm{d}\tau}{\sqrt{t - \tau}} \right\} \mathrm{d}\tau \right] \tag{32}$$

The second term represents the unsteady contribution that can be important when the frequency associated with vorticity and/or relative velocity becomes significant compared with the diffusive frequency ν_f/d^2. Asmolov and McLaughlin [30] derived an expression for an unsteady Saffman force in frequency space whereby lift can be represented by the first term of Eq. (32) multiplied by an integral term I^*, which is a function of the relative velocity frequency normalized by the fluid shear rate ϕ. The functional dependence on ϕ was obtained numerically and also approximated with an analytical functional, whereby the real part of I^* approaches unity for $\phi \ll 1$ (i.e., slow oscillations tend to the steady-state solution) but reduces significantly at higher frequencies (e.g., to about $1/10$ for $\phi \approx 10$). Simulations of particle dynamics in rotating flows by Lim et al. [31] indicate that the history portion of the lift is often negligible, but can be significant for high frequencies and small values of ρ_p/ρ_f.

For finite Re_p values, there is no analytical solution and so one must rely primarily on experiments and simulations. For the unsteady-drag component, Mei and Adrian [32] showed that the history influence decays more rapidly as a function of time once convective effects are taken into account (as Re_p increases); a result consistent with previous experimental studies. Numerical simulations at finite Reynolds numbers were used to develop a kernel that describes the transition from the creeping-flow $t^{-1/2}$ dependence at short times [similar to that noted in the second term of Eq. (32)] to the convective t^{-2} dependence at long times. A similar result may be expected for the unsteady component of the lift force. Wakaba and Balachandar [33] examined the unsteady component of the lift for a solid particle in a uniform shear, but with a constant acceleration in the relative velocity for a finite duration, with Re_p ranging from 5–125. They found that the unsteady-lift kernel at finite

Re_p was substantially smaller than the creeping-flow predictions of Asmolov and McLaughlin [30], a result consistent with the unsteady-drag behavior at finite Re_p. Wakaba and Balachandar [33] also proposed a model for the unsteady-lift kernel overall reduction that yields an effectively inviscid lift history force with a decay that scales with the convective time (instead of the diffusive time). However, they were not able to establish a quantitative model for an oscillating force that also appeared, nor did they examine conditions of deceleration, unsteady shear, or particle rotation. As such, significant work is needed to understand the unsteady-lift component for generalized fluid vorticity, spin and Reynolds number conditions.

VI. Conclusions

A comprehensive review of existing experimental data was conducted to determine lift behavior for solid spherical particle lift under shear, spin, or shear and spin. For linear shear with no spin at small Reynolds numbers, the lift in creeping flow was well-predicted by the McLaughlin [13] correction to the theoretical Saffman lift. This correction also proved reasonable up to particle-relative Reynolds numbers (Re_p) of 50, beyond which the lift coefficient tended to negative values. Kurose and Komori [15] attributed this to flow separation occurring on two places on the rear of the sphere, which led to a downward force for both the pressure and viscous components. An empirical fit was found to reasonably reproduce the resolved-surface simulations as a function of shear rate. For particles in vortical (solid-body rotation) flow, the theoretical Heron-lift coefficient for creeping flow proved reasonable for Re_p values as high as 100, and only positive lift was observed.

For particles spinning in a uniform flow relative to the particle (no vorticity), it is well known that the Rubinow and Keller [17] theory for creeping-flow conditions tends to overpredict the lift once finite particle Reynolds number conditions are considered. Because there were no previous studies that were able to predict the lift dependency on Re_p and relative spin rate (normalized by the relative velocity and particle diameter), a lift model was developed herein that robustly and quantitatively captures the lift for Re_p values as high as 1000. At much higher Reynolds numbers but still subcritical conditions (Re_p ranging from 46,000 to 100,000), negative lift coefficients were observed for particles at subcritical conditions. This was related to wake unsteadiness and was separately modeled as a function of the normalized spin rate. At higher supercritical Re_p values (at which the boundary layer became turbulent), the lift coefficient was found to again become positive.

As suggested by Bagchi and Balachandar [16] and others, conditions with both particle spin and linear shear were found to be reasonably predicted by a simple linear combination of the two separate forces for moderate Reynolds numbers (e.g., up to 40). This result, coupled with an empirical model that accounts for equilibrium spin rates at both zero and finite Re_p values, could be used to estimate the overall particle torque in combined spin and shear at steady-state conditions. The unsteady component of lift has also been investigated by several researchers. This component can be significant for large transients associated with the cross product of the relative velocity and the shear vector, but the unsteady influence is reduced at finite Reynolds numbers.

Finally, the impact of flow vorticity and particle rotation on particle drag were considered in the Appendix. Forr small Reynolds numbers, there is a theoretical increase in drag due to flow rotation, but the effects of flow shear and spin are negligible. For moderate-to-high Re_p values, drag is found to increase for both shear or spin conditions, for which empirical relations can be employed. However, the experimental evidence is insufficient to provide robust quantitative predictions for larger Re_p values, and only qualitative trends were identified.

Appendix A: Drag Modification due to Shear or Spin

The well-known definition of the drag coefficient C_D can be written in terms of the total drag force as

$$\boldsymbol{F}_D \equiv -\frac{\pi}{8} d^2 \rho_f C_D w \boldsymbol{w} \tag{A1}$$

Measurements in the range have shown that C_D below the critical Reynolds number (approximately 250,000) is well-represented by the expression given by Clift et al. [23], which is accurate to within 6% of experiments:

$$C_{D,Re_p} = \left[\frac{24}{Re_p}\left(1 + 0.15 Re_p^{0.687}\right)\right] + \frac{0.42}{1 + (42{,}500/Re_p^{1.16})} \tag{A2}$$

The term in square brackets is also known as the Schiller–Naumann [34] drag expression, which is quite accurate up to a moderate Reynolds number of 800. Note that the drag given by Eqs. (A1) and (A2) represents the time-averaged component for $Re_p > 200$, because some force unsteadiness results from the unsteady separated wake region.

The impact that freestream vorticity and particle rotation have on particle drag is considered herein. For particles subjected to vorticity, the two common idealizations for the surrounding flow are solid-body rotation ω_{rot} or linear shear ω_{shear}. For a particle in a solid-body rotation vortex at the creeping-flow limit, Heron et al. [2] determined that the drag increases as

$$C_{D,\text{vortex}} = \frac{24}{Re_p}\left(1 + \frac{5}{14}\sqrt{\omega^*_{\text{vortex}}\, Re_p/2}\right) \tag{A3}$$

This theoretical correction assumes small vorticity levels, and so it is not clear whether a significant correction occurs at large rotation rates or larger Reynolds numbers. However, experiments by Sridhar and Katz [35] for contaminated bubbles in a vortex flow at $20 < Re_p < 80$ and $0.04\ \omega^*_{\text{vortex}} < 0.1$ indicated no influence of rotational vorticity on the drag coefficient, suggesting that the effect is confined to smaller Re_p values.

For the case of linear shear, Saffman [1] found that the drag, to leading order, is simply equal to the Stokes drag (i.e., $f_{\text{shear}} = 1$). This lack of influence of vorticity on drag approximately extends to Reynolds numbers as high as 10, based on resolved-surface simulations of solid particles (Dandy and Dwyer [36] and Bagchi and Balachandar [16]). At higher Reynolds numbers, resolved-surface simulations yield drag increases for particles in shear, as shown in Fig. A1, which can be approximated for $Re_p \le 500$ and $\omega^*_{\text{shear}} \le 0.8$ as

$$\frac{C_D}{C_{D,\omega=0}} = 1 + 0.00018\, Re_p (\omega^*_{\text{shear}})^{0.7} \tag{A4}$$

However, caution should be used when employing these empirical corrections, because they are based on a limited set of conditions with no experimental verification.

For particle rotation at the small Reynolds limit with linearized inertia terms, Rubinow and Keller [17] found that there is no effect of spin on particle drag; that is, the Oseen correction is recovered. For

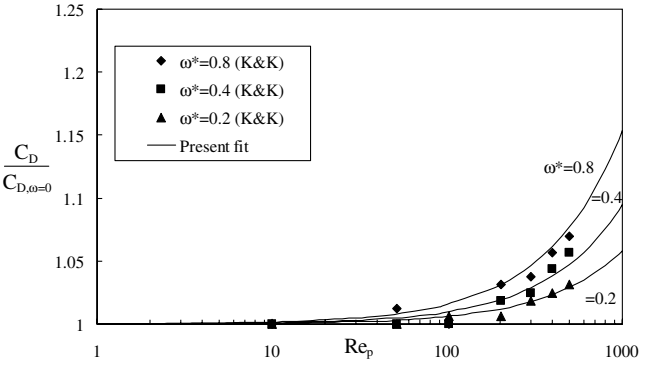

Fig. A1 Drag coefficient sensitivity to shear of the surrounding flow for solid particles based on data of Kurose and Komori [15] and predictions of Eq. (A4).

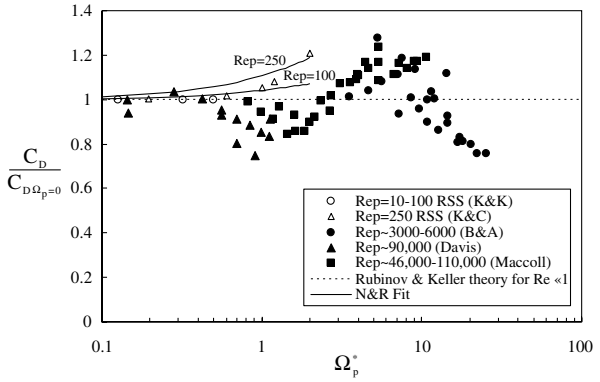

Fig. A2 Drag coefficient sensitivity to particle spin, based on the experiments of Maccoll [20], Davies [21], and Barkla and Auchterlonie (B&A) [12], the RSS of Kurose and Komori (K&K) [15] and Kim and Choi (K&C) [47], and the fit of Niazmand and Renksizbulut (N&R) [37] [Eq. (A5)]. The Kim and Choi [47] results are for spin in the relative velocity direction, whereas all the others are for spin perpendicular to the relative velocity.

particle spin at higher Re_p values, there were several experimental and computational studies, as shown in Fig. A2. There appears to be a negligible impact of spin on drag for $Re_p < 100$ and $\Omega_p^* < 0.5$, beyond which increases arise. To describe these, Niazmand and Renksizbulut [37] developed an empirical correlation for the effect of particle spin and "blowing" on drag for $Re_p < 300$ and $\Omega_p^* < 1$, which is given by

$$\frac{C_D}{C_{D,\Omega=0}} = \left(1 + \frac{\Omega_p^*}{2}\right)^{Re_p/1000} \left(1 + 20\frac{|u_{\dot{m}}|}{w}\right)^{-0.2\,\mathrm{sign}(u_{\dot{m}})} \qquad \text{(A5)}$$

The second term on the RHS includes the ratio of the radial surface velocity $u_{\dot{m}}$ to the particle relative velocity. This velocity ratio is often called the blowing number and serves to reduce the effective drag for positive (blowing) surface velocity and increases it for negative (suction) surface velocity. This correlation of Eq. (A5) generally agrees with other RSS spinning studies, as shown in Fig. A2. It also reasonably agrees with the blowing resolved-surface simulations of Cliffe and Lever [38] and the creeping-flow solution for blowing and suction given by Dukowicz [39]. However, experimental data for spinning or blowing impact on drag at moderate Re_p values conditions are lacking. At much higher Reynolds numbers and spin rates, both drag decreases (for $\Omega_p^* < 2$ or $\Omega_p^* > 15$) and increases (for $4 < \Omega_p^* < 12$) were observed, as shown in Fig. A2. These can be significant (as much as $\pm 20\%$), but the scatter in the data prevents a robust quantitative correction. As such, Crowe et al. [24] suggested simply using the uniform flow drag coefficient for spinning particles with the caveat that this is approximate.

References

[1] Saffman, P. G., "The Lift on a Small Sphere in a Slow Shear Flow," *Journal of Fluid Mechanics*, Vol. 22, 1965, pp. 385–400. doi:10.1017/S0022112065000824; Corrigendum, Vol. 31, No. 2, 1968, p. 624.

[2] Heron, I., Davis, S., and Bretherton, F., "On the Sedimentation of a Sphere in a Centrifuge," *Journal of Fluid Mechanics*, Vol. 68, No. 2, 1975, pp. 209–234. doi:10.1017/S0022112075000778

[3] Young, J., and Leeming, A., "A Theory of Particle Deposition in a Turbulent Pipe Flow," *Journal of Fluid Mechanics*, Vol. 340, June 1997, pp. 129–159. doi:10.1017/S0022112097005284

[4] Ramirez, L. E. S., Lim, E. A., Coimbra, C. F. M., and Kobayashi, M. H., "On the Dynamics of a Spherical Scaffold in Rotating Bioreactors," *Biotechnology and Bioengineering*, Vol. 84, No. 3, 2003, pp. 382–389. doi:10.1002/bit.10778

[5] Leal, L. G., "Particle Motions in a Viscous Fluid," *Annual Review of Fluid Mechanics*, Vol. 12, 1980, pp. 435–476. doi:10.1146/annurev.fl.12.010180.002251

[6] Drew, D. A. "Mathematical Modeling of Two-Phase Flow," *Annual Review of Fluid Mechanics*, Vol. 15, 1983, pp. 261–291. doi:10.1146/annurev.fl.15.010183.001401

[7] Magnaudet, J., and Eames, I., "The Motion of High-Reynolds-Number Bubbles in Inhomogeneous Flows," *Annual Review of Fluid Mechanics*, Vol. 32, 2000, pp. 659–708. doi:10.1146/annurev.fluid.32.1.659

[8] Tomiyama, A., Tamai, H., Zun, I., and Hosokawa, S., "Transverse Migration of Single Bubbles in Simple Shear Layers," *Chemical Engineering Science*, Vol. 57, 2002, pp. 1849–1858. doi:10.1016/S0009-2509(02)00085-4

[9] Wang, C. T., "Free Molecular Flow over a Rotating Sphere," *AIAA Journal*, Vol. 10, No. 5, 1972, pp. 713–714.

[10] Volkov, A. N., "The Aerodynamic and Heat Properties of a Spinning Spherical Particle in Transitional Flow," *6th International Conference on Multiphase Flow (ICMF 07)*, Paper S2_Mon_C6, 2007.

[11] Auton, T. R., "The Lift Force on a Spherical Body in a Rotational Flow," *Journal of Fluid Mechanics*, Vol. 183, Apr. 1987, p. 199. doi:10.1017/S002211208700260X

[12] Barkla, H. M., and Auchterlonie, L. J., "The Magnus or Robins Effect on Rotating Spheres," *Journal of Fluid Mechanics*, Vol. 47, No. 3, 1971, pp. 437–448. doi:10.1017/S0022112071001150

[13] McLaughlin, J. B., "Inertial Migration of a Small Sphere in Linear Shear Flows," *Journal of Fluid Mechanics*, Vol. 224, Mar. 1991, pp. 261–274. doi:10.1017/S0022112091001751

[14] Mei, R., Klausner, J. F., and Lawrence, C. J., "A Note on the History Force on a Spherical Bubble at Finite Reynolds Number," *Physics of Fluids*, Vol. 6, No. 1, 1994, pp. 418–420. doi:10.1063/1.868039

[15] Kurose, R., and Komori, S., "Drag and Lift Forces on a Rotating Sphere on a Linear Shear Flow," *Journal of Fluid Mechanics*, Vol. 384, No. 1, 1999, pp. 183–206. doi:10.1017/S0022112099004164

[16] Bagchi, P., and Balachandar, S., "Effect of Free Rotation on Motion of a Solid Sphere," *Physics of Fluids*, Vol. 14, No. 8, 2002, pp. 2719–2737. doi:10.1063/1.1487378

[17] Rubinow, S. I., and Keller, J. B., "The Transverse Force on Spinning Spheres Moving in a Viscous Liquid," *Journal of Fluid Mechanics*, Vol. 11, No. 3, 1961, p. 447. doi:10.1017/S0022112061000640

[18] Tanaka, T., Yonemura, S., and Tsuji, Y., "Experiments of Fluid Forces on a Rotating Sphere and Spheroid," *Proceedings of the 2nd KSME-JSME Fluids Engineering Conference*, Vol. 1, 1990, p. 366.

[19] Tri, B. D., Oesterle, B., and Deneu, F., "Premiers Resultants Sur la Portance D'Une Sphere en Rotation aux Nombres de Reynolds Intermediaries," *Comptes Rendus de l'Académie des Sciences, Série II: Mécanique, Physique, Chimie, Sciences de l'Univers, Sciences de la Terre.*, Vol. 311, 1990, p. 27.

[20] Macoll, J. H., "Aerodynamics of a Spinning Sphere," *Journal of the Royal Aeronautical Society*, Vol. 32, 1928, pp. 777–798.

[21] Davies, J. M., "The Aerodynamic of Golf Balls," *Journal of Applied Physics*, Vol. 20, 1949, pp. 821–828. doi:10.1063/1.1698540

[22] Sawicki, G. S., Hubbard, M., and Stronge, W., "How to Hit Home Runs: Optimum Baseball Bat Swing Parameters for Maximum Range Trajectories," *American Journal of Physics*, Vol. 71, No. 11, 2003, pp. 1152–1162. doi:10.1119/1.1604384

[23] Clift, R., Grace, J. R., and Weber, M. E., *Bubbles, Drops and Particles*, Academic Press, New York, 1978.

[24] Crowe, C., Sommerfeld, M., and Tsuji, Y., *Multiphase Flows with Droplets and Particles*, CRC Press, Boca Raton, FL, 1998.

[25] Salem, M. B., and Oesterle, B., "A Shear Flow Around a Spinning Sphere: Numerical Study at Moderate Reynolds Numbers," *International Journal of Multiphase Flow*, Vol. 24, No. 4, 1998, pp. 563–585. doi:10.1016/S0301-9322(97)00082-7

[26] Happel, J., and Brenner, H., *Low Reynolds Number Hydrodynamics*, Noordhoff International, Leyden, The Netherlands, 1973.

[27] Lin, C. J., Perry, J. H., and Scholwater, W. R., "Simple Shear Flow Round a Rigid Sphere: Inertial Effects and Suspension Rheology," *Journal of Fluid Mechanics*, Vol. 44, No. 1, 1970, p. 1. doi:10.1017/S0022112070001659

[28] Basset, A. B., "On the Motion of a Sphere in a Viscous Liquid," *Philosophical Transactions of the Royal Society of London, Series A: Mathematical and Physical Sciences*, Vol. 179, 1888, pp. 43–63. doi:10.1098/rsta.1888.0003

[29] Coimbra, C. F. M., and Kobayashi, M. H., "On the Viscous Motion of a Small Particle in a Rotating Cylinder," *Journal of Fluid Mechanics*, Vol. 469, Oct. 2002, pp. 257–286. doi:10.1017/S0022112002001829

[30] Asmolov, E. S., and McLaughlin, J. B., "The Inertial Lift of an Oscillating Sphere in a Linear Shear Flow Field," *International Journal of Multiphase Flow*, Vol. 25, No. 4, 1999, pp. 739–751. doi:10.1016/S0301-9322(98)00063-9

[31] Lim, E. A., Coimbra, C. F. M., and Kobayashi, M. H., "Dynamics of Suspended Particles in Eccentrically Rotating Flows," *Journal of Fluid Mechanics*, Vol. 535, July 2005, pp. 101–110. doi:10.1017/S0022112005004908

[32] Mei, R., and Adrian, R. J., "Flow Past a Sphere with an Oscillation in the Free-Stream and Unsteady Drag at Finite Reynolds Number," *Journal of Fluid Mechanics*, Vol. 237, Apr. 1992, pp. 323–341. doi:10.1017/S0022112092003434

[33] Wakaba, L., and Balachandar, S., "History Force on a Sphere in a Weak Linear Shear Flow," *International Journal of Multiphase Flow*, Vol. 31, No. 9, 2005, pp. 996–1014.

[34] Schiller, L., and Naumann, A. Z., "Über die Grundlegenden Berechungen bei der Schwerkraftaufbereitung," *VDI-Zeitschrift*, Vol. 77, 1933, pp. 318–320.

[35] Sridhar, G., and Katz, J., "Drag and Lift Forces on Microscopic Bubbles Entrained by a Vortex," *Physics of Fluids*, Vol. 7, No. 2, 1995, pp. 389–399. doi:10.1063/1.868637

[36] Dandy, H. A., and Dwyer, D. S., "Some Influences of Particle Shape on Drag and Heat Transfer," *Physics of Fluids A*, Vol. 2, No. 12, 1990, pp. 2110–2118. doi:10.1063/1.857797

[37] Niazmand, H., and Renksizbulut, M., "Surface Effects on Transient Three-Dimensional Flows Around Rotating Spheres at Moderate Reynolds Numbers," *Computers and Fluids*, Vol. 32, No. 10, 2003, pp. 1405–1433. doi:10.1016/S0045-7930(02)00115-9

[38] Cliffe, K. A., and Lever, D. A., "Isothermal Flow Past a Blowing Sphere," *International Journal for Numerical Methods in Fluids*, Vol. 5, No. 8, 1985, pp. 785–802.

[39] Dukowicz, J. K., "An Exact Solution for the Drag of a Sphere in Low Reynolds Number Flow with Strong Uniform Blowing or Suction," *Physics of Fluids*, Vol. 25, No. 7, 1982, pp. 1117–1118. doi:10.1063/1.863875

[40] Cherukat, P., McLaughlin, J. B., and Graham, A. L., "The Inertial Lift on a Rigid Sphere Translating in a Linear Shear Flow Field," *International Journal of Multiphase Flow*, Vol. 20, No. 2, 1994, pp. 339–353. doi:10.1016/0301-9322(94)90086-8

[41] Narciri, M. A., "Contribution a l'Etude des Forces Exercees Par un Liquide sur une Bulle de Gaz: Portance, Masse Ajoutee et Interactions Hydrodynamiques," Ph.D. Thesis, L'ecole Centrale de Lyon, Lyons, France, 1992.

[42] Felton, K., and E. Loth, "Spherical Bubble Motion in a Turbulent Boundary Layer," *Physics of Fluids*, , Vol. 13, No. 9, Sept. 2001, pp. 2564–2577. doi:10.1063/1.1388051

[43] Bagchi, P., and Balachandar, S., "Shear Versus Vortex-Induced Lift on a Rigid Sphere at Moderate Re," *Journal of Fluid Mechanics*, Vol. 473, Dec. 2002, pp. 379–388. doi:10.1017/S0022112002002628

[44] Tsuji, Y., Morikawa, Y., and Mizuno, O., "Experimental Measurements of the Magnus Force on a Rotating Sphere at Low Reynolds Numbers," *Journal of Fluids Engineering*, Vol. 107, No. 9, 1985, pp. 484.

[45] Jeffrey, R. C., and Pearson, J. R. A., "Particle Motion in a Laminar Vertical Tube Flow," *Journal of Fluid Mechanics*, Vol. 22, No. 4, 1965, pp. 721–735. doi:10.1017/S0022112065001106

[46] Poe, G. G., and Acrivos, A., "Closed-Streamline Flows Past Rotating Single Cylinders and Spheres: Inertia Effects," *Journal of Fluid Mechanics*, Vol. 72, No. 4, 1975, pp. 605–623. doi:10.1017/S0022112075003187

[47] Kim, J., and Choi, H., "Laminar Flow Past a Sphere Rotating in the Streamwise Direction," *Journal of Fluid Mechanics*, Vol. 465, July 2002, pp. 354–386.

[48] Legendre, D., and Magnaudet, J, "Lift Force on a Bubble in a Viscous Linear Shear Flow," *Journal of Fluids Mechanics*, Vol. 368, 1998, pp. 81–126.

[49] Nathan, A. M., Hopkins, J., Chong, L., and Kaczmarski, H., "The Effect of Spin on the Flight of a Baseball," International Sports Engineering Conference, Munich, July 2006 http://arxiv.org/abs/physics/0605041.

[50] Briggs, L. J., "Effects of Spin and Speed on the Lateral Deflection (Curve) of a Baseball and the Magnus Effect for Smooth Spheres" *American Journal of Physics*, Vol. 27, 1959, pp. 589–596.

[51] Watts, R. G. and Ferrer, R., "The Lateral Force on a Spinning Sphere: Aerodynamics of a Curve Ball" *American Journal of Physics*, Vol. 55, No. 1, 1987, pp. 40–44.

[52] Tani, I., "Baseball's Curved Balls" *Kagaku*, Vol. 20, 1950, pp. 405–409.